Phase separation and up-hill diffusion in the ordered α2 compound of a γ- Ti-Al-Nb alloy

Heike Gabrisch[1], Tobias Krekeler[2], Uwe Lorenz[1], Marcus Willi Rackel[1], Martin Ritter[2], Florian Pyczak[1], Andreas Stark[1]

[1]Helmholtz-Zentrum Geesthacht, Department of Metal Physics, Max-Planck-Str.1, 21502 Geesthacht, Germany

[2]Technische Universität Hamburg, Betriebseinheit Elektronenmikroskopie BEEM, Eißendorfer Straße 42, 21073 Hamburg, Germany

Abstract
γ-TiAl alloys are intermetallic materials that are designed for applications in air craft engines. Oftentimes alloying elements are added to improve the corrosion resistance and mechanical properties. Here we investigate microstructural changes that take place when Nb is added to a binary γ-TiAl alloy. Previous studies of the alloy Ti-42Al-8.5Nb have shown that upon Nb addition the orthorhombic O-phase forms out of the parent α_2 phase within the alloy's microstructure. During annealing Nb segregates to the newly formed O-phase while Al and Ti partition to the remaining α_2-like matrix phase. The changes these newly formed O-phase domains undergo with time at elevated temperature are not known. Here we use Transmission Electron Microscopy techniques to monitor the distribution of Nb and the size of O-phase domains during long-term annealing between 1 week and 4 weeks at 550°C. The results show that the size of O-phase domains shrinks with annealing time. At the same time the Nb concentration remains largely constant or possibly shows a small decrease.

1. Introduction
γ-Titanium aluminides have a high specific strength at elevated temperatures, which makes them an attractive structural light-weight material for applications in aircraft engines. At an Al-content of 40-45 at.-% the main constituents in the microstructure of these alloys are the hexagonal α_2 phase (Ti_3Al, D019) that forms out of the high temperature hcp α phase and the tetragonal y phase (TiAl, L12) that precipitates within α_2 grains during further cooling. A negligible percentage of β_0 phase (or ω_0 phase) may form at triple junctions if the content of β-stabilizing elements (e.g. Nb, Mo, Ta) is sufficiently high. During cooling a near lamellar microstructure forms, where the γ and α_2 phases are aligned parallel to their close packed lattice planes in lamellar (α_2 + γ) colonies. The crystallographic orientation relationship has been described by Blackburn [1].
Third generation γ-TiAl-alloys are often alloyed with niobium for improved creep strength and oxidation resistance [2]. The addition of Nb can introduce an additional, orthorhombic phase to the alloy's microstructure that forms inside α_2 lamellae in the temperature range between 450 and 670°C. The thermal stability range of this O-phase is limited: above 700°C it re-transforms to hexagonal α_2 phase. Furthermore, its formation can be largely suppressed by air-cooling from temperatures above 700°C.
We investigated the formation of O-phase in the alloy Ti-42Al-8.5Nb (at.-%) by in-situ heating HEXRD and studied its location within lamellar (α2+γ) colonies by TEM [3, 4]. Initial ambiguity on the nature of the orthorhombic phase was resolved and it was identified as sub-stoichiometric O-phase (Ti2AlNb, Cmcm) [5, 6]. Similar findings were reported by [7, 8]. The orthorhombic O-phase has been described for the first time much earlier by Banerjee in Nb-rich, Al-lean Ti-Al compositions and it has been studied intensely [9-11]. However until the first reports by Appel et al. it was unknown in γ-based TiAl-alloys and it was a novelty to identify O-phase at this small, nm size scale within α2 lamellae. By now the existence of O-phase is accepted and more details of its appearance – the size and the shape of O-phase domains including the distribution of Nb- are investigated [12, 13].
In the present paper the microstructure of two annealed states is compared (T= 550°C, duration: 1 week and 4 weeks). We show that Nb agglomerates in small domains separated by Ti and Al rich channels (1 week). The lattice within these Nb-rich domains is distorted with respect to the hexagonal lattice of α_2 and is identified as the orthorhombic O-phase. In contrast, the Nb-lean channels inbetween domains show only little distortion. After 4 weeks of annealing the O-phase domains split into smaller islands separated by wider channels. At the same time, there is only little change in the Nb concentrations observed in the domains.

2. Experimental
The alloy Ti-42Al-8.5Nb was produced by powder metallurgy starting from pure elements following the method described in [14]. After compacting by hot-isostatic pressing (200 MPa, 1250 °C, 2 h, Ar atmosphere) the alloy was annealed at 550 °C for 1 week (168 h) and for 4 weeks (672 h) to form the orthorhombic phase. Specimens for TEM investigations were prepared by standard methods, see [3].
TEM and HAADF STEM investigations were performed at the Helmholtz-Zentrum in Geesthacht with the Titan 80-300 kV and the CM 200 operated at 300 kV and at 200 kV, respectively. Atomic resolution HAADF STEM and EDX mapping were employed to characterize the size/shape and elemental distribution within α_2/O-phase lamellae. The atomic resolution HAADF STEM images were obtained at the CNMS, at Oakridge National Laboratory using the Nion UltraSTEM 100 dedicated aberration-corrected STEM at 100 kV. Elemental EDX mapping with the signals Al-K, Nb-L, Ti-K was performed at the BEEM facility of the Technical University Hamburg using a SuperX detector system attached to an FEI-Talos F200XTEM operated at 200 kV with a probe current of 1 nA.
The average size of O-phase domains was measured in Adobe® photoshop on a grid superimposed onto STEM HAADF

images. The image magnification was 160,000x (0.85 nm pixels size) and 320,000x (0.42 nm pixels size) and 5 images of different lamellar colonies were measured in each annealing state. The size of the grid was chosen so that every domain was measured only once in vertical and horizontal image direction. The total number of measurements was 351 and 343 for the 1 week and the 4 week annealing state. For the measurement of matrix channel width intensity-scaled Nb maps were used (image intensity proportional to Nb wt.-%, 0.4 nm pixel size). The measurements were performed in Digital Micrograph™ on intensity profiles oriented perpendicular to channels between Nb rich regions. Per annealing state 13 measurements were performed. For the 1 week specimen Nb maps recorded from 2 lamellar colonies were used; for the 4 week specimen measurements were performed in one grain. At the same time, the Nb concentrations were measured in a 5 nm wide region above of the line profile as illustrated in Fig. 5.

3. Results and Discussion

An overview of the alloy's microstructure consisting of lamellar ($\alpha_2 + \gamma$) colonies is given in the SEM image in Fig. 1a. The schematic sketch in Fig. 1b illustrates the orientation relationship between the phases inside the lamellar colonies where the α_2-(0001) plane is parallel to the α_2/γ interface. The O-phase that is investigated here forms within the α_2 phase lamellae by a displacement of atom positions in α_2-(0001) planes. As a result of the displacement, the lattice of the O-phase is distorted with respect to the lattice of the parent α_2 phase. All following micrographs are taken in α_2-[0001] viewing direction. The α_2 lamellae are called α_2/O-phase lamellae hereafter because after the heat treatment at 550°C both phases co-exist in them.

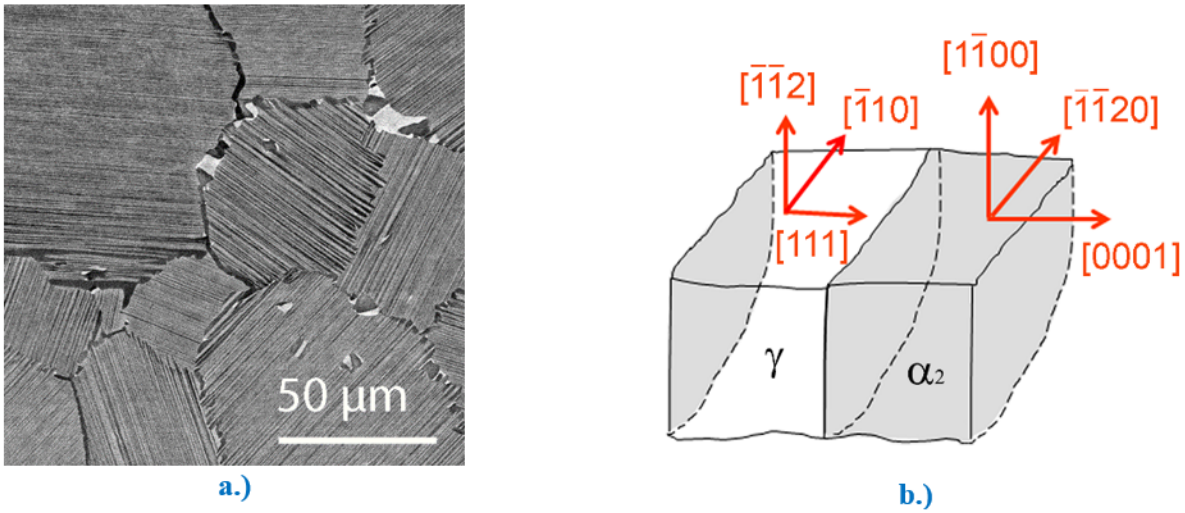

Fig. 1 : Overview of the alloy's microstructure. a.) SEM image of lamellar (α2 + γ) colonies. b.) Orientation relationship between the phases in lamellar colonies.

Microstructure after 1 week of annealing at 550°C

Fig. 2 shows a series of images of α_2/O-phase lamellae in [0001] projection at increasing magnifications. In Fig. 2a a TEM-bright field image shows a section of a lamellar colony with parallel lamellae of γ and α_2/O-phase. A striking feature are the dark and bright facets that appear inside α_2/ O-phase lamellae. These facets are differently tilted regions of the crystal lattice that appear brighter or darker depending of the number of electrons scattered away from the transmitted beam. In Fig. 2b a HAADF STEM image shows an enlarged section of an α_2/O-phase lamella together with neighboring γ-phase. Under the image conditions chosen (L= 195mm) the image is mostly formed by z-contrast. The facets, which appear under diffraction contrast in Fig. 1a, are no longer visible. Instead a pattern of dark lines on a brighter background is discernable that suggests that heavy and light elements concentrate in different regions (in z-contrast elements with a higher atomic number z appear brighter). In Fig. 2c, taken in atomic resolution HAADF STEM mode, the darker and brighter regions of the α_2/O-phase lamellae can be seen more clearly. In the bright regions the lattice is elongated along <1120> directions of the α_2 lattice reducing the six-fold hexagonal α_2 symmetry to the two-fold symmetry of an orthorhombic lattice. These bright regions are O-phase domains. The darker regions between the O-phase domains are formed by lighter elements. Close inspection also shows that these regions are less distorted than the O-phase domains. Based on the almost hexagonal appearance and the predominance of Al and Ti (see below) we call these regions α_2-like matrix even though the symmetry is not perfectly hexagonal. There is no sharp border between O-phase domains and α_2-matrix but rather a smooth transition.

The nature of the z-contrast observed in HAADF STEM images can be identified in the EDX maps in Fig. 3. Elemental maps taken with the signals of Al-K, Ti-K and Nb-L are shown in Figs. 3a-c. A comparison to Fig. 2b. and 2c. confirms agglomerations of Al and Ti in α_2-like matrix channels whereas Nb concentrates within O-phase domains.

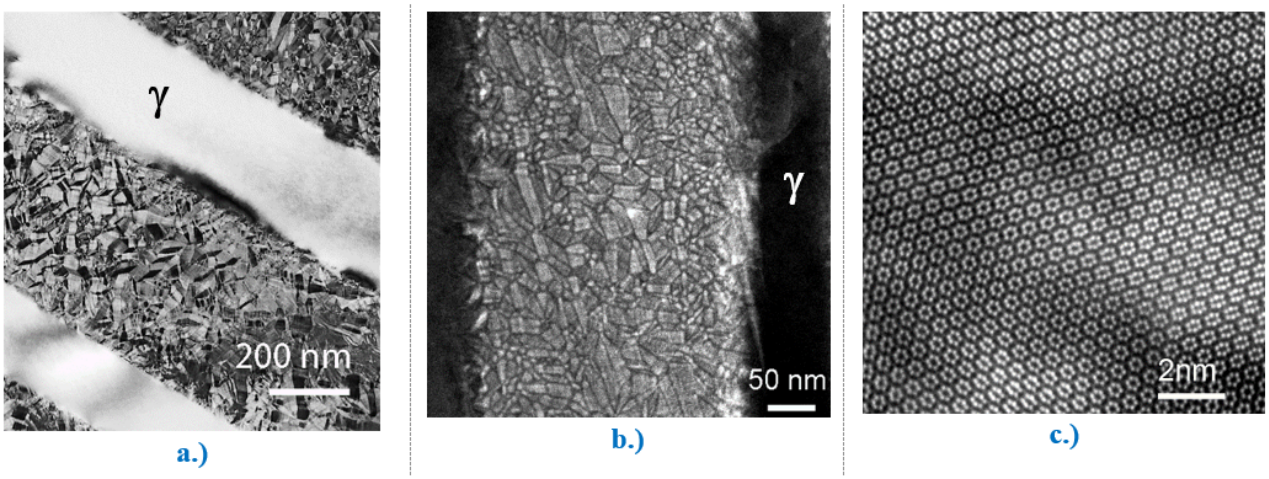

Fig. 2 : a.) Bright-field TEM image of a section of a lamellar colony in α_2-[0001] orientation. The bright phase is γ, the darker lamellae are a mixture of α2 and O-phase. b.) HAADF-STEM image showing finer details (dark lines) within α_2/O-phase lamella. c.) Atomic resolution HAADF-STEM image illustrating that brighter regions are more distorted than the darker regions between them.

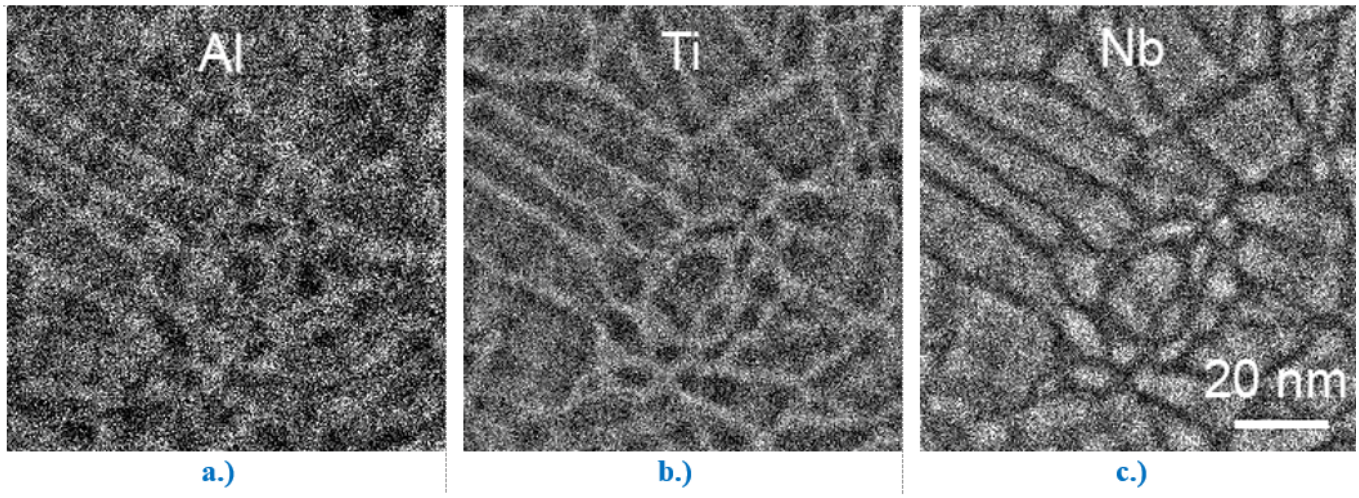

Fig. 3 : Elemental maps of ¬λ2/O-phase region in a specimen annealed at 550 °C for 1 week. The maps were recorded with the signals of : a.) Al-K, b.) Ti-K, c.) Nb-L. Bright regions correspond to higher concentrations (wt.-%).

Comparison between microstructures after 1 and 4 weeks of annealing at 550°C

With prolonged annealing time the general features of the microstructure do not change. In both annealing states Nb- rich O-phase domains are observed that are separated by α_2-like matrix channels enriched in Al and Ti. At close inspection, it appears that the size of O-phase domains and the widths of matrix channels have changed after 4 weeks of annealing. This is illustrated in Fig. 4, where Nb maps recorded after 1 week and 4 weeks of annealing are shown side by side. The inset Fig. 4a represents the annealing state after 1 week whereas the larger part of the image (Fig. 4b) corresponds to 4 weeks of annealing. Comparison shows that the larger regions in Fig. 4a are divided into smaller islands in Fig. 4b. At the same time, the channels between the bright regions appear wider.

To confirm these impressions, the average domain sizes were measured on HAADF STEM images of both annealing states. The matrix channels widths and the Nb-concentrations were measured using concentration profiles on Nb maps as illustrated in Fig. 5.

The measurements of domain sizes on STEM-HAADF images give average values of 10 nm for the 1 week annealing state and 7.0 nm for the 4 weeks annealing state. The margins of error (95% confidence interval for population mean) are 1 nm and 0.5 nm respectively (rounded). The large variation in domain sizes is in agreement with the observations in Fig. 4. There, after 1 week of annealing, elongated, rhomboidal or rectangular Nb rich regions are observed that have large aspect ratios. For comparison after 4 weeks of annealing the brighter Nb islands are smaller in size with an aspect ratio closer to one. Statistical analysis (t-test) indicates that the difference in means between the two populations is significant (p-value < 10-3). This supports the conclusion that the domain size shrank during the extra time the 4 week specimen was exposed to the annealing temperature. This result is rather surprising as one would expect continued growth with longer annealing time. The mechanism of shrinkage is splitting of domains as illustrated in Fig. 5. There, the splitting of a domain is

heralded by a darker image contrast in the center of the domain and a drop in Nb concentration at the corresponding position in the profile. The two corresponding positions are marked by arrows.

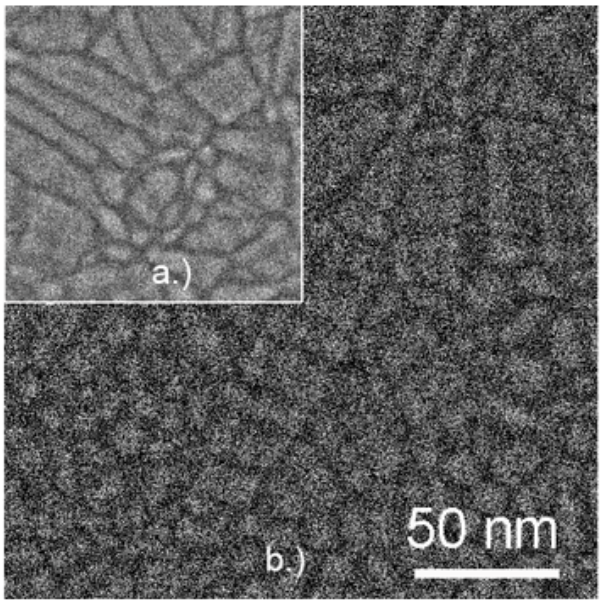

Fig. 4 : Nb maps of specimens annealed for 1 week (a.) and for4 weeks (b.). After 4 weeks of annealing the domains have split up into smaller sections and the channel width has increased.

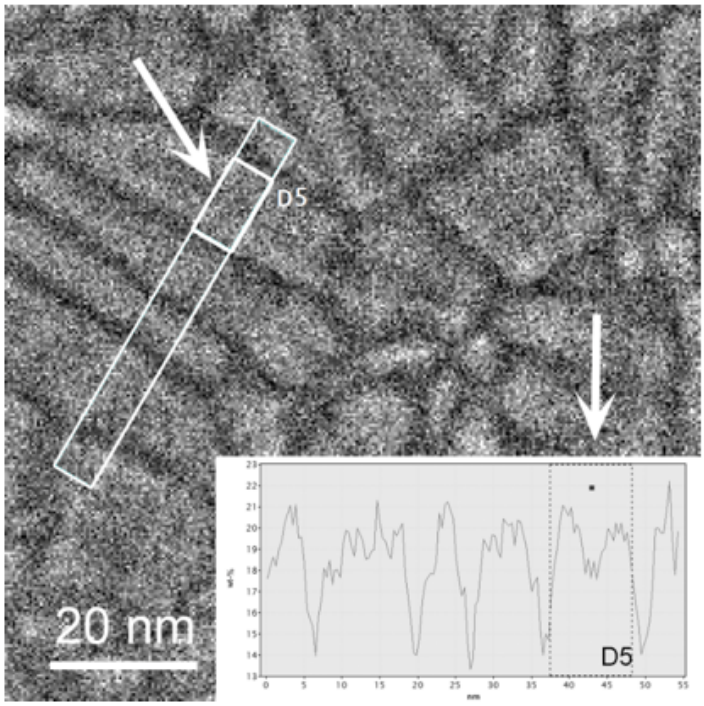

Fig 5: Illustration of the measurement of channel width (1 week, 550°C). The concentration profile in the lower corner represents the Nb concentration integrated over the length of the large rectangular region that is marked in the image. A sliding tool allows to choose a smaller section of the profile or in the image as illustrated by the smaller box within the rectangular section and the corresponding dotted lines in profile.

Table 1: Mean values for Nb concentrations (± standard deviation) in O-phase domains and matrix channels and widths of matrix channels.

(n= 13)	**Nb wt.-%-Domain**	**Nb wt.-% Channel**	**Δ Nb- wt.% Domain - channel**	**Channel width [nm]**
1 week	20 ± 1	16 ± 1	4	2 ±0.6
4 weeks	17 ± 1	11 ± 1	6	4.6 ±1.5

The results of the measurements of Nb concentrations and of matrix channel widths are summarized in table 1. The mean channel width grows from 2.1 ± 0.6 nm (standard deviation) after 1 week of annealing to 4.6 ± 0.6 nm (standard deviation) after 4 weeks annealing time. Even though the standard deviation is rather large (about 30 %) there is no overlap between the measured values. The difference is also apparent in Fig. 4.
A comparison of the Nb concentrations between the 2 annealing states shows that higher values were measured in both- matrix channels and domains- after the shorter annealing time. This is unexpected. 20 ± 1 wt.-% are measured in domains after 1 week of annealing compared to 17 ± 1 wt.-% after 4 week of annealing. Similarly, 16 ± 1 wt.-% are measured in matrix channels after 1 week of annealing compared to 11 ± 1 wt.-% after 4 weeks of annealing. Likely explanations are that the Nb concentrations differ between separate grains or that Nb segregates to the interface with γ or moves into the γ-phase. These points will have to be checked. In previous measurements the difference in Nb concentration between lamellar colonies was 0.8 – 3.2 wt.-% which is close to the observed difference in the present experiments [3]. A factor that certainly influences the present results is the irregular shape of the Nb enrichment within the O-phase domains. In the 1 week specimen Nb rich ridges appear near the domain edge in Fig. 4a but not after 4 weeks in Fig. 4b. This may explain higher Nb values in the 1 week specimen. Clearly, more measurements are needed and the measured Nb concentrations should be regarded with caution. Nevertheless, the finding that there is no distinct increase in Nb concentration in O-phase domains after 4 weeks of annealing is remarkable. Especially considering the history of the microstructural evolution: The Nb concentration was homogeneous in the starting material and after 8 hours of annealing at 550°C. It should be mentioned that after 8 hours of annealing O-phase had already formed [12]. Only after annealing for 1 week at 550°C Nb up-hill diffusion to O-phase domains was observed (Figs. 2, 3c). In the continuation of this trend one might expect even higher values after 4 weeks of annealing. But this is not found here. For comparison to the present measurements on elemental maps the Nb concentration measured in larger regions within α_2/O-phase lamellae in this alloy was 9 at.-% or 19 wt.-% in previous experiments [3]. The stoichiometric O-phase Ti2AlNb has a Nb concentration of 43 wt.-%.

4. Conclusions

We monitored size and composition of O-phase domains in α_2/O-phase-lamellae in the alloy Ti-42Al-8.5Nb after annealing at 550°C for a duration of 1 and 4 weeks. Atomic resolution HAADF-STEM images and elemental maps show that Nb rich O-phase domains are embedded in an α_2-like matrix in both annealing states. The orthorhombic, Nb-rich lattice of the O-phase shows a distinct distortion while the lattice in the α_2–like matrix channels is the less distorted- almost hexagonal. The size of O-phase domains shrinks with prolonged annealing time by a splitting mechanism. Surprisingly, the Nb concentrations within O-phase domains in both annealing states remain roughly constant or even show a small decrease. Taken together, the microstructural evolution between 1 and 4 weeks of annealing at 550°C indicates that in absence of a concentration gradient, Nb diffusion in this system might be influenced by internal stresses that act between O-phase domains.

5. Acknowledgements

Atomic resolution HAADF STEM imaging was conducted using the Nion UltraSTEM 100 (U100) dedicated aberration-corrected STEM at the Center for Nanophase Materials Sciences, which is a DOE Office of Science User Facility.

6. References

[1] M.J. Blackburn, Science, Technology, and Application of Titanium (1970) 633-643.
[2] F. Appel, M. Oehring, and R. Wagner, Intermetallics 8 (2000) 1283-1312.
[3] H. Gabrisch, et al., Acta Materialia 135 (2017) 304- 313.
[4] M.W. Rackel, et al., Acta Materialia 121 (2016) 343-351.
[5] F. Appel, M. Oehring, and J.D.H. Paul, Advanced Engineering Materials 8 5 (2006) 371-376.
[6] F. Appel, M. Oehring, and J.D.H. Paul, Materials Science and Engineering A-Structural Materials Properties Microstructure and Processing 493 1-2 (2008) 232-236.
[7] L. Song, et al., Journal of Alloys and Compounds 618 (2015) 305-310.
[8] G.-d. Ren and J. Sun, Acta Materialia 144 (2018) 516- 523.
[9] D. Banerjee, et al., Acta metall. 36 4 (1988) 871-882.
[10] L.A. Bendersky, A. Roytburd, and W.J. Boettinger, Acta metall. mater. 42 7 (1994) 2323-2335.
[11] K. Muraleedharan, et al., Metallurgical Transactions A 23A (1992) 401-415.
[12] H. Gabrisch, et al., THERMEC'2018: 10th International Conference on Processing and Manufacturing of Advanced Materials, M.I. R. Shabadi, M. Jeandin, C. Richard and Tara Chandra, Editor. (2018), Scientific Net: Paris, France. p. 741-746.
[13] G.-d. Ren, et al., Acta Materialia 165 (2019) 215- 227.
[14] R. Gerling, H. Clemens, and F.P. Schimansky, Advanced Engineering Materials 6 1-2 (2004) 23-38.